Catechol as a corrosion inhibitor of steel in an alkaline medium containing chlorides

V.E. Kasatkin,* I.V. Kasatkina, L.P. Kornienko, I.G. Korosteleva, V.N. Dorofeeva and N.N. Andreev

A.N. Frumkin Institute of Physical Chemistry and Electrochemistry, Russian Academy of Sciences, Leninsky pr. 31, 119071 Moscow, Russian Federation
**E-mail: vadim_kasatkin@mail.ru*

Abstract

There is information about the use of diatomic phenol $C_6H_4(OH)_2$ as a corrosion inhibitor of steel reinforcement in concrete. Catechol (*ortho*-dihydroxybenzene) has the greatest effectiveness among the three isomers for inhibiting corrosion of steel. However, the mechanism of its action has not been sufficiently studied. In this publication, a study of the corrosion behavior of unalloyed steel in a model solution of a pore liquid of concrete with a high chloride content has been performed. The electrochemical behavior of catechol under cathodic and anodic polarization on a platinum electrode is investigated. It has been found that in the cathode section of the polarization curve, in the presence of catechol, currents due to the reduction of dissolved oxygen are significantly reduced. With anodic polarization more positive than E = –170 mV (Ag/AgCl), an asymmetric peak is observed associated with the oxidation of catechol and the manifestation of unsteady diffusion of its oxidation products. From the polarization curves on steel it is evident, that the addition of catechol effectively reduces the oxygen recovery currents and affects the ratio of the oxidized iron forms (Fe(II)/Fe(III), but it does not affect the depassivation potential of steel at the same pH level of the solution with and without an inhibitor. By the method of linear polarization resistance, the dynamics of the corrosion rate from the concentration of catechol was studied. An increase in the inhibitory effect with an increase in the additive concentration to 1 g/L and its decrease at 5 g/L of catechol was found. The mechanism of the inhibitor effect is discussed.

Received: July 18, 2023. Published: August 2, 2023 doi: 10.17675/2305-6894-2023-12-3-12

Keywords: *steel, model concrete pore fluid, inhibitor, catechol, corrosion.*

1. Introduction

Several publications on the use of phenol derivatives as inhibitors for the protection of metals from corrosion in natural conditions, including steel reinforcement in concrete, have appeared [1–6]. Among them, diatomic phenols with the chemical formula $C_6H_4(OH)_2$ are most often mentioned. These compounds exist as three isomers: Pyrocatechin (catechol, *ortho*-dihydroxybenzene), resorcinol (*meta*-dihydroxybenzene) and hydroquinone (*para*-dihydroxybenzene). All of these isomers have strong antioxidant properties. They are widely

used in the chemical industry in the production of dyes, medicinal substances [7], as well as reducing agents. In particular, these compounds are the components of photo-developers [8].

Catechol (acronym CC) has the strongest inhibitory effect against corrosion of steel [9] and aluminum [2] among these three isomers. There is evidence [10] that this substance is also used as an additive in concrete mixtures to give them a plasticizing effect at a concentration of 0.003–0.05% CC. Preliminary studies have shown its effectiveness in reducing corrosion of carbon steel in an alkaline medium with a high chloride content, which is a model of pores fluid in concrete. However, the mechanism of its action required additional studies [11]. This publication is devoted to solving these issues.

2. Experimental

2.1. Materials

Rolled carbon steel 08PS (an analog of A620 steel) 0.2 mm thick was used. The shape and design of the samples will be described below for each of the research methods. Before starting electrochemical measurements, the surface of the samples was sanded on abrasive paper (M40), degreased and washed with water.

The corrosion behavior of steel was studied in a model solution simulating a concrete pores liquid with high chloride content. A basic solution without an inhibitor (blank solution) had the composition: 1 g/L CaO + 30 g/L NaCl (pH = 12.2). Chemical grade reagents were used. Immediately before the start of the experiment, a calculated suspension of CC was added to it and thoroughly mixed and pH was adjusted[1] to 12.2 (as in the solution without additives). The experiments were carried out under conditions of natural aeration at room temperature.

2.2. Instruments and techniques

All electrochemical studies were carried out using universal IPC series potentiostats[2] (Russia) [12]. The measurements were done in three-electrode cell at a potentiostatic control. A saturated chloride-silver electrode connected to the cell *via* a salt bridge and a Luggin capillary was used as the reference electrode. The potentials in the article are given relative to this electrode. The auxiliary electrode was made of titanium wire.[3]

2.2.1 Polarization curves

To study the nature of electrochemical processes occurring on the steel surface in model solutions with different CC content, polarization curves were obtained. Polarization curves on a platinum electrode (wire area $S = 0.15$ cm^2) in blank solutions and with CC additives

[1] Using NaOH solution.

[2] The IPC-Pro and IPC-Micro models were used.

[3] We have previously checked that the titanium auxiliary electrode in the range of recorded currents is not inferior to the platinum electrode and does not disrupt the potentiostat operation. Unlike platinum, the titanium electrode has no catalytic activity and does not change the properties of inhibitors.

were used to evaluate the electrochemical behavior of the inhibitor in a wide potential range. They were started from the open circuit potential (OCP) in the cathodic direction with a potential sweep (5 mV/s) to the region of hydrogen release and further in the anodic direction to the potential E = +600 mV.

Rectangular steel samples measuring 2×2 cm with current leads embedded in glass tubes with epoxy resin were used to obtain polarization curves. These curves were taken in the same way as described above, but the sweep in the anodic direction was limited by the potential of intensive corrosion of steel. The polarization curves were recorded 2 min after immersion the sample in the solution and repeated again after holding it for 30 and 60 min.

2.2.2 Linear polarization resistance (Corrosion meter)

To assess the change in the corrosion rate over time, the linear polarization resistance method was implemented with a help of specially developed computer software CorrMeter for IPC series potentiostats [13]. These measurements were carried out similarly to those previously published [14, 15]. The measurement procedure was a combination of two-minute sample exposures without polarization (and OCP registration) and short-term anodic polarization at the potential E_{OCP} + 10 mV. During the polarization, the current I was measured and the polarization resistance was calculated as the ratio 10 mV/I. These cycles were repeated continuously for periods from several days to a month. The design of the samples was the same as described above, and they were connected to the potentiostat as a working electrode. The working surface of the samples was 10 mm below the liquid level in the cell.

3. Results and Discussion

3.1. Polarization curves

When using CC as an inhibitor of steel corrosion, a variety of electrochemical processes can occur in the system, relating both to reactions involving the metal itself and its oxides, and redox processes associated with the inhibitor. Therefore, preliminary experiments on platinum electrode were carried out in order to study the electrochemical behavior of CC proper in an alkaline chloride-containing solution modeling a concrete pores liquid. Figure 1 shows the polarization curves in blank model solution that does not contain an inhibitor (red curve a) and with the addition 0.1 g/L of CC.

The yellow curve b was obtained immediately after the introduction of the inhibitor into the solution, and the green and blue curves c and d correspond to the state of the system 30 and 60 min after the start of the experiment, *i.e.* they allow us to assess the changes occurring with CC over time.

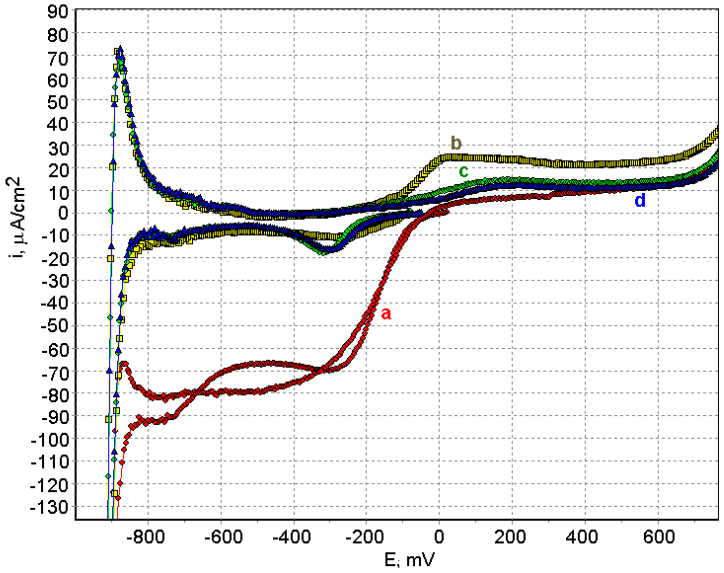

Figure 1. Polarization curves on Pt electrode in a model solution with CC additives: (a) blank solution, (b) 0.1 g/L CC after 2 min, (c) 0.1 g/L CC after 30 min, (d) 0.1 g/L CC after 60 min.

Platinum is thermodynamically stable in the potential range studied, hence, the current changes are caused by reactions with the components of the solution rather than with the electrode material. Thus, the cathodic currents at potentials from 0 to –850 mV, forming a plateau, both at the forward and reverse potential sweep, is associated with the reduction of oxygen in the air saturating the solution:

$$O_2(\text{gas}) + 2H_2O + 4\bar{e} = 4OH^- \quad (1)$$

At higher cathodic potentials, hydrogen is released by the reaction[4]:

$$H_2O + \bar{e} = 1/2\,H_2(\text{gas}) + OH^- \quad E = -0.91\ \text{V} \quad (2)$$

In the right part of the polarization curve in the range from 0 mV to +600 mV, no significant currents are registered, *i.e.* in this potential region, the behavior of platinum approaches an ideally polarizing electrode.

The form of polarization curves changes significantly with CC addition to the solution. At the potentials of oxygen reduction reaction (1) the currents decrease by an order of magnitude, which indicates a decrease in O_2 concentration in solution due to the reaction with CC, a powerful antioxidant. According to [7], the reaction with oxygen proceeds by a homolytic mechanism (*i.e.* in the bulk of the solution) with the formation of oxanthrene-2,3-dione:

[4]All Nernst potentials are calculated for reactions [16] for a solution with pH = 12.2 with respect to the silver chloride reference electrode.

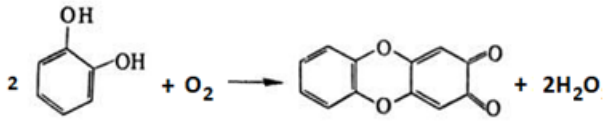

(3)

In the presence of CC, the hydrogen release potential does not change, however, the peak of hydrogen desorption is more clearly manifested compared to the blank solution at the anodic sweep. This is probably due to the reduction to a minimum of the oxygen content dissolved in the solution. Similar peaks usually appear on platinum in deaerated solutions.

In the potentials region more positive than −100 mV in the solution with CC, the formation of an anodic current wave is observed, which is absent in the blank solution. This wave is caused by the beginning of the reaction of CC oxidation, at the first stage of which 1,2-benzoquinone is formed by heterolytic mechanism [7]:

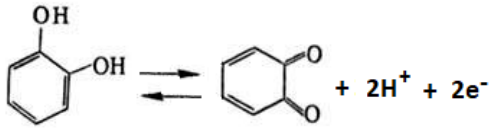

(4)

Obviously, in an alkaline environment, the equilibrium of this reaction will be shifted towards the oxidation of CC.

The anodic current forms a plateau (diffusion restrictions on CC transportation to the electrode surface) and, when higher potentials are reached, the current increases due to the onset of oxygen release and/or the manifestation of deeper CC oxidation reactions.

Comparing the appearance of curves b, c and d it can be concluded that over time there are no noticeable changes in the cathodic currents in the oxygen reduction region (the antioxidant effect is sufficient to suppress oxygen), but the height of the anodic wave of inhibitor oxidation decreases markedly, signaling a decrease in the concentration of CC over time.

From Figure 2 and 3 representing similar polarization curves at concentrations of CC 0.5 g/l and 1 g/L, respectively, it is obvious that with an increase in the concentration of the additive, there is no proportional increase in the amplitude of the anodic current wave. The peak of the anodic current and its deeper decline at the exit to the plateau are becoming more and more distinctive. The formation of an asymmetric peak on the potentiodynamic curve is associated with the manifestation of unsteady diffusion of the components of the electrochemical reaction and is described by the Randles–Sevcik equation:

$$i_{max} = 0.443nFC(nFvD/(RT))^{1/2} \quad (5)$$

where i_{max} is the maximum current density at the peak (A/cm^2), n is the number of electrons in the reaction, F is the Faraday constant, v is the potential sweep rate (V/s), C is the reagent concentration (mol/cm^3), D is the diffusion coefficient (cm^2/s), T is the temperature (K), and R = 8.314 J K^{-1}·m^{-1}.

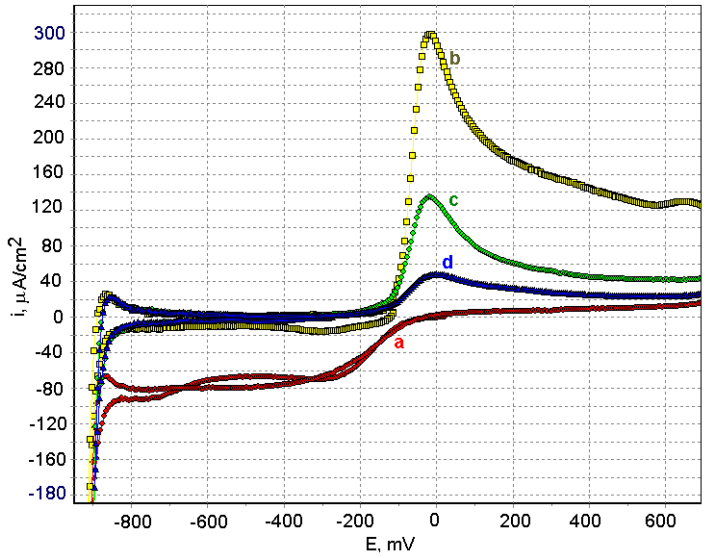

Figure 2. Change in the polarization curve with the addition of 0.5 g/L CC over time: (a) blank solution, (b) 0.5 g/L CC after 2 min, (c) 0.5 g/L CC after 30 min, (d) 0.5 g/L CC after 60 min.

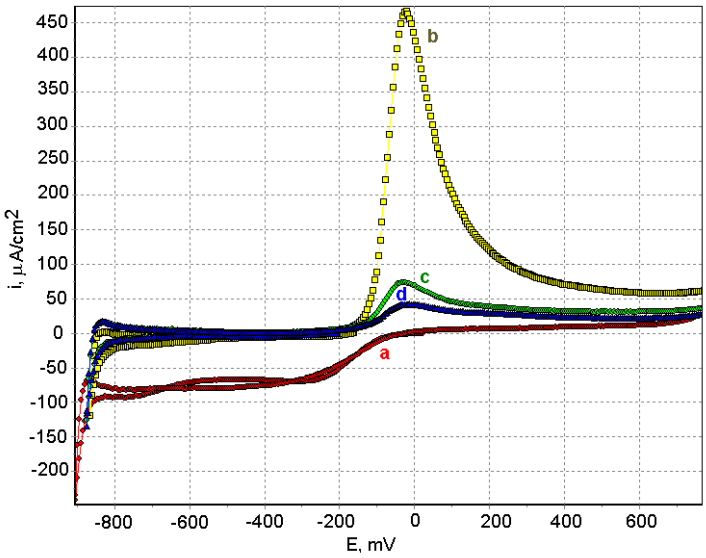

Figure 3. Change in the polarization curve with the addition of1 g/L CC over time: (a) blank solution, (b) 1 g/L CC after 2 min, (c) 1 g/L CC after 30 min, (d) 1 g/L CC after 60 min.

We observed a rapid decrease in currents when at the repeated curves over time, and the rate of decrease increases greatly with an increase in the concentration of CC. It is obvious that with a constant potential sweep rate, the decrease in currents as the solution ages may be due to both a decrease in CC concentration due to its oxidation and a decrease in its diffusion coefficient due to changes in the properties of the solution at the electrode surface. If we assume that the diffusion coefficient does not change over time, then it turns

out that at the initial content 1 g/L of CC, its concentration should decrease in 30 min by 7 times! It is more likely that the oxidation of CC is accompanied by the accumulation of poorly soluble resinous oxidation products of CC on the electrode, which complicate the diffusion of the reagent and can block the active surface of the electrode (changing the actual current density). Estimated calculations using equation (5) [17] using a virtual calculator [18], confirmed that the observed results can be explained only with a simultaneous decrease in *C* and *D*.

Since the reaction rate of homogeneous oxidation (3) is proportional to the CC content, with an increase in its concentration, the effect of accumulation of the resinous reaction product in solution increases. This product inhibits diffusion and, therefore, should reduce the peak current, which is observed in our experiments. Indeed, after experiments in more concentrated solutions, a resinous film was observed on the surface of Pt electrode, which should be regularly removed by special treatment.[5]

Thus, CC in an alkaline solution undergoes electrochemical oxidation at the anodic potentials about –100 mV. In the cathodic region, we did not observe an increase in currents that could be attributed to the reverse reaction of the reduction of oxidized CC. At the same time, a sharp decrease in cathodic currents indicates that CC effectively reduces the concentration of dissolved oxygen in the electrolyte. This can help to increase the corrosion resistance of metals for which the process proceeds by the mechanism of oxygen depolarization.

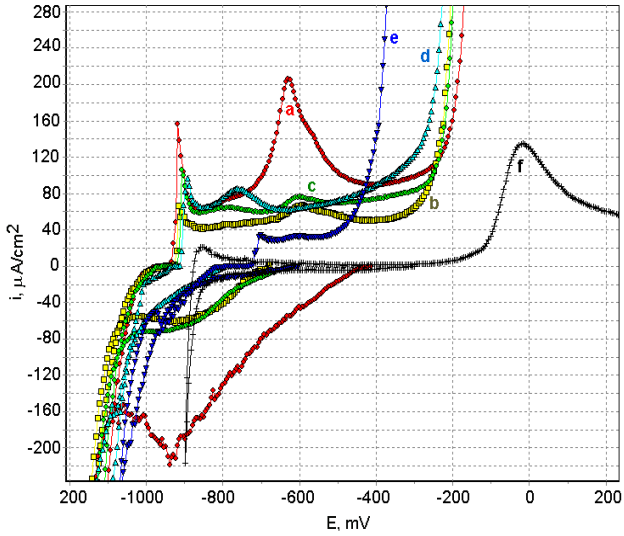

Figure 4. Polarization curves on steel obtained 30 minutes after the addition of CC to model solution: (a) blank solution, (b) 0.1 g/L CC, (c) 0.5 g/L CC, (d) 1 g/L CC, (e) 5 g/L CC. For comparison see curve (f): 0.5 g/L CC on Pt electrode.

[5]After treating Pt electrode with water and acetone, it was placed in the blank solution and subjected to multiple cyclic polarization between the hydrogen and oxygen release potentials until the CVA curve was the same as for pure Pt.

Figure 4 shows the polarization curves on steel obtained in a background solution with CC additives. On the cathode branch of the curve, in the blank solution in the range from –400 mV to –1100 mV, the reduction of dissolved oxygen (1) and surface oxides occurs and then hydrogen is released (2). On the anode branch of the polarization curve, characteristic areas can be associated with reactions:[6]

$$Fe(OH)_2 + 2\bar{e} = Fe + 2OH^- \quad E = -0.97 \text{ V} \tag{6}$$

$$Fe(OH)_3 + \bar{e} = Fe(OH)_2 + OH^- \quad E = -0.66 \text{ V} \tag{7}$$

In other words, the first anodic current peak is associated with the oxidation of iron by reaction (6) and the formation of an oxide-hydroxide layer of poorly soluble Fe(II) compounds on the surface, and the second peak corresponds to Fe(III) oxide formation by reaction (7). The oxidized iron compounds in an alkaline medium occurs in the form of poorly soluble oxides and hydroxides that block the electrode surface and limit the anodic current. This explains the appearance of currents plateaus on curves. At lower anodic potentials, Fe(II) compounds predominate: $Fe(OH)_2$ and Fe_3O_4. They are oxidized to Fe(III), *i.e.* to $Fe(OH)_3$ and γ-Fe_2O_3, when the potentials of reaction (7) are reached. The latter compounds have lower solubility and provide stronger protection of the metal from corrosion [19]. When the potential of the steel becomes more positive than –200 mV, the surface oxides no longer provide passivation and sharp increase in the anodic current occurs, signaling the destruction of the metal with the formation of pitting.

In the presence of CC additives, the shape of polarization curves on steel changes. In the cathode region, as in experiments on platinum, there is a decrease in currents in the oxygen reduction region. This effect is enhanced at the higher additive concentrations. The potentials of the hydrogen evolution reaction (2) shift more strongly with an increase in the concentration of CC. This inhibitor belongs to phenols with a slightly acidic reaction, so an increase in its concentration leads to a slight decrease in alkalinity.[7] This explains the observed change in the potential of the pH-sensitive reaction (2) according to Nernst's equation.

The shape of the anode branches of the polarization curves in solutions with an inhibitor changes compared to the blank curve. Thus, at low concentrations 0.1 and 0.5 g/L of CC, the passivation currents decrease, while the characteristic potentials of the curve sections practically do not change. At a concentration 1 g/L of CC, the reaction potential (6) does not change much, but for the reaction (7) it becomes lower by 150 mV, which indicates an increase in the Fe(II)/Fe(III) ratio due to a growing in the antioxidant properties of the solution. In the solution with 5 g/L of CC, the reaction potential (6) becomes significantly anodic due to a strong decrease in pH. Although the passivation currents at the same time

[6] The Nernst potentials are calculated for reactions on iron for the solution with pH = 12.2 relative to the silver chloride reference electrode (assuming equimolar concentrations of the reagents).

[7] In these experiments, no pH correction was performed after the addition of catechol.

turn out to be the smallest, the extent of the passive region in potential is noticeably narrowed and the steel depassivation occurs already at $E = -500$ mV.

In general, from Figure 4 it is evident, that the addition of CC to the model solution without pH correction at the level of the blank solution (pH = 12.2) leads to a progressive decrease in the potential of steel depassivation with an increasing in the additive concentration. In other words, in this case CC does not expand the range of passivity potentials but, on the contrary, narrows it. Its inhibitory effect is manifested in a decrease in the current density in the passive region, as well as in a weakening of the oxygen depolarizing reaction. It is also obvious from Figure 4 that the sharp increase in anodic currents is due precisely to the oxidation of steel, and not CC, since the latter, judging by the curve on platinum, is oxidized at higher anodic potentials.

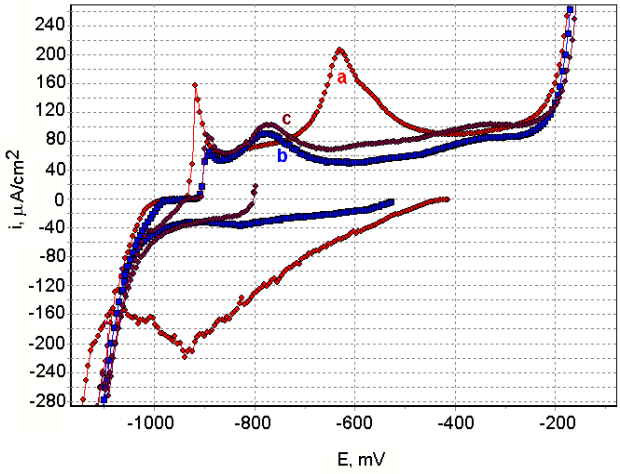

Figure 5. Polarization curves on steel in model solution with pH = 12.2: (a) blank solution, (b) 5 g/L CC, (c) 10 g/L CC.

A similar experiment with high concentrations of CC additives (5 and 10 g/L) to a model solution with the pH adjusted to 12.2, is shown in Figure 5. In this case the shape of the anode branches of polarization curves with CC practically does not differ. In addition, the depassivation potentials of steel in the blank solution and with CC are just the same, *i.e.* they do not depend on the CC content, but on the pH level.

Thus, the addition of CC the model pores solution enhances the reducing properties, causing a decrease in the concentration of dissolved oxygen (and thereby contributes to the inhibition of corrosion with oxygen depolarization). Also, the presence of an antioxidant in the system contributes to the predominance of more reduced forms of iron compounds over oxidized ones. In other words, the surface of steel is enriched with less protective forms of Fe(II) to the detriment of more stable Fe(III) compounds that contribute to the expansion of the passive potential range, as happens with the addition of nitrites [9, 14, 19].

3.2. Linear polarization resistance (Corrosion Meter)

It is convenient to study the change in the corrosion state of the system in real time using the method of linear polarization resistance. In this case, the metal sample is placed in a corrosive environment without the imposition of external polarization and it's OCP is measured. Then it is periodically polarized for a short time with an anodic shift of the OCP by dE = 10 mV. The polarization resistance R_p is calculated by the magnitude of the polarization current dI:

$$R_p = dE / dI \tag{8}$$

Since the corrosion current I_{corr} is inversely proportional to the polarization resistance [20]:

$$I_{corr} = b_a \cdot b_c / 2.3(b_a + b_c) \cdot R_p = C1 / R_p \tag{9}$$

where b_a, b_c are Tafel's constants for the anodic and cathodic sections of the polarization curve, according to Faraday's law, it is possible to calculate the mass losses of metal K per unit surface S:

$$K = k \cdot I_{corr} / S \tag{10}$$

where k is the electrochemical equivalent.

Thus, taking into account certain assumptions, the corrosion rate of the metal and the polarization resistance can be related by the proportionality coefficient $C2$[8]. In this case, the measurement can be performed with low DC polarization [13]:

$$K = C2 / R_p \tag{11}$$

Of course, polarization resistance measurements cannot replace direct corrosion experiments based on the classical weight loss method (gravimetry). Moreover, the numerical results of corrosion rate obtained by linear polarization resistance may differ from classical gravimetry. They are evaluative and can only be compared with the results obtained in a similar experiment. However, if the same measurement regime is observed, they allow monitoring the state of corrosion systems over time and promptly comparing the behavior of samples at different concentrations of the inhibitor.

The time change in the corrosion rate of steel samples in model solutions with different CC content obtained by measuring the linear polarization resistance is shown in Figure 6a. Simultaneously measured open circuit potentials for these samples are shown in Figure 6b.

[8]The numerical value of this coefficient depends on the nature of the metal, the units of measurement and the method of conducting the experiment.

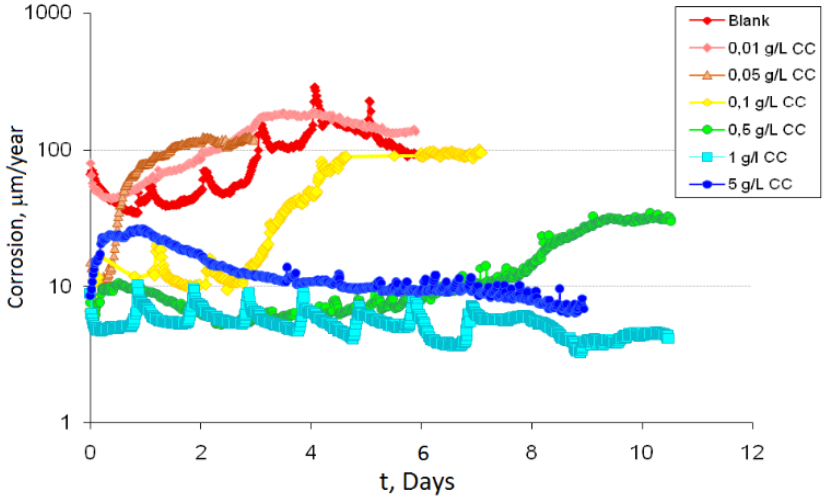

Figure 6a. Change in corrosion rate of steel over time when exposed in solutions with different concentrations of CC.

Discussing the results obtained, it should be noted that the experiments were carried out in rooms whose temperature was not strictly constant. In some experiments, the temperature could periodically change from 17° to 27°C when illuminated by the Sun. Therefore, fluctuations in parameters with an obvious circadian rhythm are well manifested on some curves.

It was found that at a lowest concentration 0.01 g/L of CC, the change in the corrosion rate and potential over time generally differs little from the blank solution without additives. At such low concentration of CC, no noticeable corrosion inhibition is observed, and the potential steadily decreases, reaching $E = -700$ mV after 6 days.

With an increase in the concentration of CC to 0.05 g/L, the corrosion rate turns out to be several times lower for several hours compared to the blank solution, but after a day the inhibitory effect disappears.

By doubling the concentration of CC to 0.1 g/L, the inhibitory effect persists for 3.5 days, but then the corrosion rate increases and reaches "blank solution values". It is interesting to note that, despite the almost cessation of the inhibitory effect after 4–5 days, the potential of steel in a solution with the addition of CC turns out to be 100 mV more anodic, although it continues to decrease.

At CC concentration of 0.5 g/L, the corrosion rate was an order of magnitude lower than in a solution without additives. Such a strong inhibition persisted for a week, then the protective effect decreased slightly. The OCP potential remained at the level from –450 to –500 mV throughout the experiment.

The strongest inhibitory effect was found at 1 g/L of CC concentration. For 10 days, the corrosion rate remained at the level of 7–10 µm/year, *i.e.* more than an order of magnitude lower compared to the blank solution.

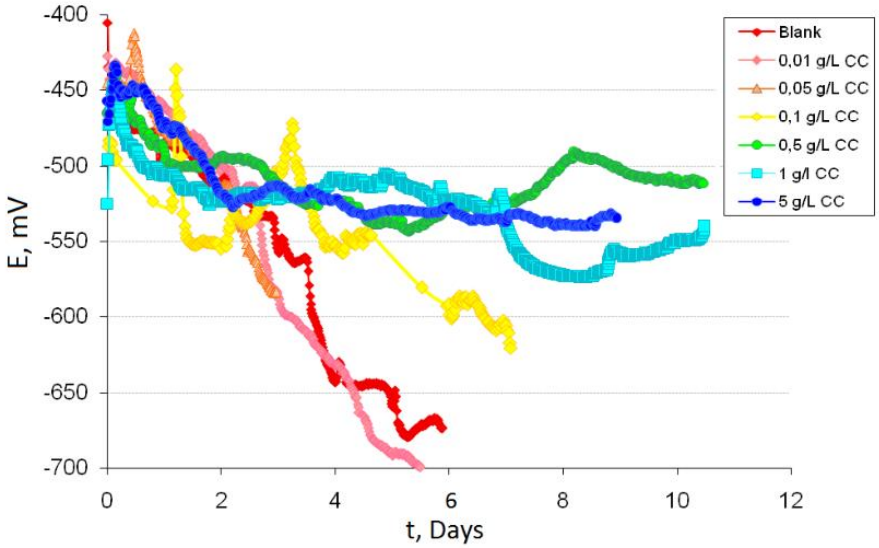

Figure 6b. Change in OCP of steel over time when exposed in solutions with different concentrations of CC.

At the highest CC concentration of 5 g/L, the corrosion rate during the experiment decreased significantly, although to a lesser extent than with the addition of 1 g/L of CC. At the same time, for concentrations from 0.5 to 5 g/L of CC, the nature of the potential change over time turned out to be almost the same, *i.e.* it decreased slightly from –450 to –550 mV.

Thus, a relatively long-lasting inhibitory effect is observed at concentrations of CC above 0.5 g/L. With a lower content, the effective concentration of the additive is rapidly reduced due to the oxidation reaction with dissolved oxygen (which is clearly noticeable by the darkening of the solution and the formation of a resinous film on the surface of the solution and the walls of the vessel (Figure 7) and, consequently, is insufficient for long-term inhibition of steel corrosion.

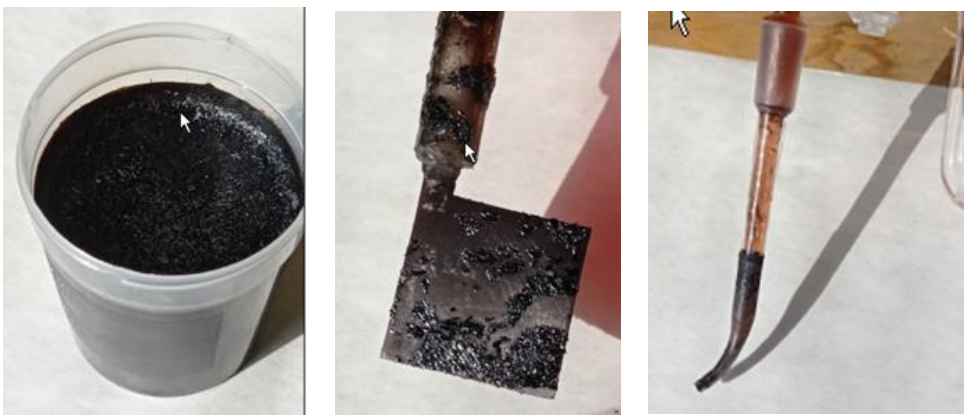

Figure 7. Photos of the cell, electrode and Luggin capillary after 1 month of exposure in a solution with 1 g/L CC.

If we take the solubility of oxygen in 3% NaCl for 7 mg/L [21], its molar concentration will be 0.22 mmol. At a CC concentration of 0.05 g/L or 0.45 mmol, the stoichiometric ratio of the reaction components (3) is approximately observed. Thus, the complete oxidation of CC to oxanthrene-2,3-dione occurs in one day. At higher concentrations of CC, as long as its non-oxidized form is present in the solution, the oxygen level remains low and corrosion of steel with oxygen depolarization is inhibited. As CC is consumed, oxygen re-saturates the solution, and corrosion increases.

Thus 0.05 g/L of CC is the threshold concentration. With a lower content of CC, it will not be enough to completely reduction of dissolved oxygen in a given volume of solution. With a higher initial content of CC in solution, its non-oxidized form will remain in solution longer, providing counteraction to oxygen coming from the atmosphere and, consequently, increasing the duration of the "protective period". Thus, at 1 g/L of CC the corrosion rate remains at the level about 7–10 μm/ year for at least 10 days. It is interesting to note that with an increase in the concentration of CC to 5 g/L, the corrosion rate at the initial moment is as low as at the concentration 1 g/L, but during the first day its increase and subsequent gradual decrease are observed. At the same time, the corrosion rate turns out to be slightly higher compared to the experiment with a lower concentration of the inhibitor.

It is obvious that at CC concentrations above 0.05 g/L in the initial period, the oxygen reaction is reliably blocked and free (non-oxidized) CC can interact with steel corrosion products, for example, Fe(III) compounds, causing their reduction to Fe(II), which has less protective ability. The higher the concentration of CC, the stronger it has a reducing effect on surface oxides. As time passes, the concentration of free CC decreases, and its activity decreases, although for a long time it is enough to block oxygen coming from the atmosphere. Therefore, there must be an optimal concentration of the inhibitor, which is a compromise between the neutralization of oxygen supply to the solution and the reducing effect on surface iron oxides. For comparison, Table 1 presents the results of estimating corrosion rates by polarization resistance a day after the start of the experiment. From these data, it is obvious that the optimal concentration was 1 g/L of CC.

Based on these data, it is possible to estimate the coefficients of corrosion inhibition γ under the action of an inhibitor by the formula:

$$\gamma = K_0 \diagup K_{\text{inh}} \tag{12}$$

where K_0 and K_{inh} are, respectively, the corrosion rates in a blank solution and with an inhibitor.

The degree of protection of steel under the action of the *Z* inhibitor can be calculated by the formula:

$$Z = (K_0 - K_{\text{inh}}) \diagup K_0 \cdot 100\% \tag{13}$$

Table 1. The corrosion rate obtained by polarization resistance method on the next day after the start of the experiment.

Concentration of CC, g/L	Corrosion rate		γ	*Z*, %
	μm/year	g/(m²·day)		
0	44.8	0.97	–	–
0.01	57.3	1.24	0.78	-27.9
0.05	78.3	1.69	0.57	-74.8
0.1	10.4	0.22	4.31	76.8
0.5	9.7	0.21	4.62	78.3
1	7.2	0.16	6.22	83.9
5	25.0	0.54	1.79	44.2

3.3. Temperature dependence of corrosion rate

As mentioned above, our tests of the inhibitor effectiveness over time were carried out without strict adherence to the constancy of cell temperature. At the same time, the sun periodically fell into the room, oriented with windows to the south side. As a result, the cell with the model solution and the steel sample was subjected to heating - cooling cycles, which caused fluctuations in the corrosive current (and obtained *K* values). This is clearly noticeable by periodically repeating wave graphs of the corrosion rate over time for a blank solution and with the addition 1 g/L of CC. We took advantage of this phenomenon and measured the temperature of the solution in the cell synchronously with the corrosion rate. Since the dependence of the corrosion rate *K* on the temperature *T* is described by the Arrhenius Equation:

$$K = k_0 \cdot e^{-E/RT} \tag{14}$$

From these data, it is possible to estimate the activation energy *E* of the process causing the corrosion.

Table 2. The temperature dependence of the corrosion rate for the experiment with 1 g/L of CC.

K, μm/year	*t*, °C	*T*, K	ln *K*	$1/RT \cdot 10^{-4}$
6.65	27.0	300.0	1.895	4.01
6.39	26.0	299.0	1.855	4.02
6.44	25.0	298.0	1.863	4.04
4.49	20.0	293.0	1.502	4.11
4.97	21.0	294.0	1.603	4.09
5.15	22.0	295.0	1.639	4.08

***K*, µm/year**	***t*, °C**	***T*, K**	**ln *K***	**$1/RT \cdot 10^{-4}$**
5.74	23.0	296.0	1.747	4.06
5.90	24.0	297.0	1.775	4.05
7.18	26.0	299.0	1.971	4.02
7.41	26.0	299.0	2.003	4.02
6.43	26.0	299.0	1.861	4.02
6.05	25.0	298.0	1.800	4.04
6.09	25.0	298.0	1.807	4.04
6.10	25.0	298.0	1.808	4.04
6.99	28.0	301.0	1.944	4.00
3.60	16.0	289.0	1.281	4.16
3.70	16.5	289.5	1.308	4.15
4.27	16.5	289.5	1.452	4.15
4.51	19.0	292.0	1.506	4.12
4.85	20.0	293.0	1.579	4.11
4.75	21.0	294.0	1.558	4.09
4.99	21.5	294.5	1.607	4.08
4.75	22.0	295.0	1.558	4.08
5.17	22.0	295.0	1.643	4.08

When processing the experimental results for this experiment according to equation (14), the value of the activation energy of the process E = 41.57 kJ/mol was obtained (see Figure 8).

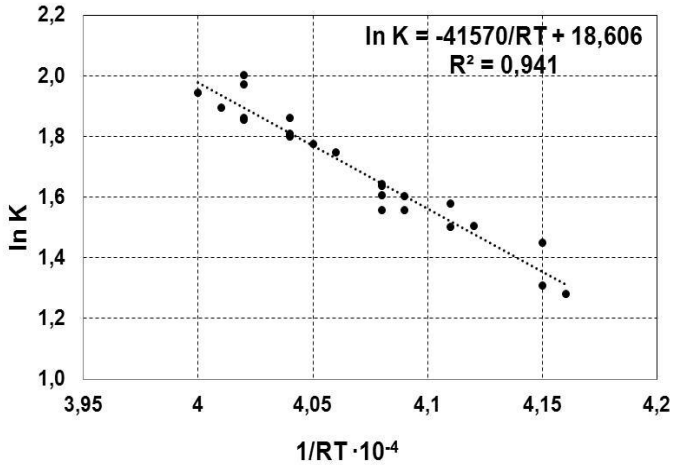

Figure 8. Processing of experimental results in Arrhenius coordinates.

Focusing on studies [22], where values $E = 38$ kJ/mol were obtained for the Fe(II)/Fe(III) oxidation reaction, we can conclude that in our case we have a value of the same level. That is, this activation energy probably refers to the oxidation of iron as the main component of steel.

4. Conclusions

The electrochemical behavior of catechol in an alkaline chloride-containing solution has been investigated. It is shown that in the presence of catechol, the concentration of dissolved oxygen decreases due to the reducing action of catechol. At the same time, catechol is consumed and its oxidation products do not have an inhibitory effect.

It was found that the potential at which a sharp increase in anodic currents occurs on steel practically does not depend on the concentration of catechol in solution and is 100 mV lower than the oxidation potential of catechol on platinum electrode. Therefore, this potential should be considered the potential of steel depassivation and pitting formation.

It was found that in the presence of catechol, the depassivation potential of steel does not depend on its concentration, provided that the pH of the solution with additives is maintained at the level of the background solution. It is shown that the inhibitory effect of catechol is not associated with the expansion of the passivation region by potentials, but is caused by a decrease in currents in the passive region.

By the method of polarization resistance, the dynamics of the change in the corrosion rate from the concentration of catechol was studied and it was found that at its concentration above 0.05 g/L, an inhibitory effect is observed, the duration of which and the degree of inhibition increases with an increase in the concentration of the additive to 1 g/L. At 5 g/L of catechol, the inhibition efficiency decreases.

The observed optimum of Catechol concentration is due to a compromise between its antioxidant activity leading to a decrease in the oxygen content in the solution and the reduction of surface oxides on steel. The first helps to reduce the rate of corrosion of steel occurring in an alkaline environment with oxygen depolarization. The second, on the contrary, reduces the protective properties of surface oxides on the metal.

In a subsequent publication, the results of corrosion tests of the developed system classical weight loss method and electrochemical impedance spectroscopy will be presented, which will allow a more complete understanding of the mechanism of action of catechol inhibitor.

Declarations of competing interests

The authors declare that they have no known competing financial interests or personal relationships that could have appeared to influence the work reported in this paper.

References

1. M. Abdallah, B.H. Asghar, I. Zaafarany and A.S. Founda, The inhibition of carbon steel corrosion in hydrochloric acid solution using some phenolic compounds, *Int. J. Electrochem. Sci*., 2012, **7**, 282–304. doi: 10.1016/S1452-3981(23)13338-4
2. J. Ryl, M. Brodowski, M. Kowalski, W. Lipinska, P. Niedzialkowski and J. Wyscka, Corrosion inhibition mechanism and efficiency differentiation of dihydroxybenzene isomers towards aluminum alloy 5754 in alkaline media, *Materials*, 2019, **12**, 3067. doi: 10.3390/ma12193067
3. D. Veys-Renaux, S. Reguer, L. Bellot-Gurlet, F. Mirambet and E. Rocca, Conversion of steel by polyphenolic model molecules: Corrosion inhibition mechanism by rutin, esculin, esculetol, *Corros. Sci*., 2018, **136**, 1–8. doi: 10.1016/j.corsci.2018.02.015
4. J.T. Gilson, D. Grove, E.S. Troscinski, O. Lawn, T.C. Curtis, C.C. Hills, R.G. Watson and L. Grange, *Process for inhibiting corrosion of metallic surfaces with cooling water containing phenol-aldehyde resins*, US Patent 3687610A 29.08.1972.
5. A.G. Mack, *Preparation of oxidation resistant metal powde*r, US Patent 5064469, 12.11.1991.
6. R.P. Kreh, V.R. Kuhn, J. Richardson, R.M. Spotnitz, Ch.G. Carter and V. Jovancicevic, *Corrosion inhibition with water-soluble rare earth chelates*, US Patent 5130052A, 14.07.1992.
7. G.I. Putsa, *Catehol, in: Chimicheskaya Encyclopedia*, 3rd edn, Bolshaya Rossiyiskaya Encyclopedia, 1992, pp.1056–1057 (in Russian).
8. V.P. Mikulin, *Photoreceptive guide*, 2rd edn, Iskusstvo, 1960, p. 74 (in Russian).
9. I.A. Gedvillo, A.S. Zhmakina, N.N. Andreev and S.S. Vesely, Effect of hydroquinone and pyrocatechin on the corrosion and electrochemical behavior of steel in a model concrete pore liquid, *Int. J. Corros. Scale Inhib*., 2019, **8**, no. 3, 560–572. doi: 10.17675/2305-6894-2019-8-3-7
10. M.E. Voronkov, A.S. Brykov, O.K. Nekrasova and S.S. Pavlov, Influence of pyrocatechol on the properties of cementless refractory concrete mixtures based on silica-containing colloidal binders, *Novye Ogneupory (Refractories and Industrial Ceramics)*, 2018, **10**, 49–52 (in Russian). doi: 10.17073/1683-4518-2018-10-49-52
11. I.A. Gedvillo, A.S. Zhmakina and N.N. Andreev, Effect of pyrocatechol on the electrochemical behavior of rusty reinforcing steel in chloride-containing concrete, *Korroz.: Mater., Zasch. (Corrosion: Materials, Protection)*, 2020, **9**, 25–29 (in Russian). doi: 10.31044/1813-7016-2020-0-9-25-29
12. V.E. Kasatkin, L.N. Solodkova and Yu.V. Kondrashov, IPC-Family Potentiostats: Practical Application in Electrochemical Methods of Investigation. Part 1. Analyzer of Organic Additives – "KORIAN-3", *Electroplat. Surf. Treat*., 2011, **19**, 27–34.
13. N.G. Anufriev and V.E. Kasatkin, New software for corrosion research based on IPC series potentiostats, *Prakt. Anticorroz. Zaschch*., 2020, **5**, 52–62 (in Russian). doi: 10.31615/j.corros.prot.2020.97.3-6

14. V.E. Kasatkin, V.N. Dorofeeva, I.V. Kasatkina, I.G. Korosteleva and L.P. Kornienko, Monitoring the effectiveness of corrosion inhibitors by electrochemical methods. Sodium nitrite as an inhibitor for the protection of steel in a model solution of the concrete pores fluid, *Int. J. Corros. Scale Inhib*., 2022, **11**, no. 1, 198–220. doi: 10.17675/2305-6894-2022-11-1-11
15. V.E. Kasatkin, V.N. Dorofeeva, I.V. Kasatkina I.G. Korosteleva, L.P. Kornienko, N.N. Andreev, I.A. Gedvillo and A.S. Zhmakina, Ascorbic acid as a corrosion inhibitor of steel in chloride-containing solutions of calcium hydroxide, *Int. J. Corros. Scale Inhib*., 2022, **11**, no. 2, 727–751. doi: 10.17675/2305-6894-2022-11-2-19
16. A.M. Sukhotin, *Handbook of Electrochemistry*, Khimiya, 1981, pp. 125–154 (in Russian).
17. B.B. Damaskin and O.A. Petrij, *Introduction to theoretical electrochemical kinetics*, 2nd edn., Vysshaya shkola, 1975, pp. 219–224 (in Russian).
18. L. Hoyos, Randles–Sevcik, *Equation Calculator*, https://www.calctool.org/physical-chemistry/randles-sevcik-equation, Accessed 01 July 2022.
19. I.L. Rozenfeld, *Corrosion Inhibition*, McGraw Hill Inc., 1982.
20. M. Stern and A.L. Geary, Electrochemical Polarization I. A Theoretical Analysis of the Shape of Polarization Curves, *J. Electrochem. Soc*., 1957, **104**, 56–63. doi: 10.1149/1.2428496
21. *Technical tables. Solubility of oxygen in fresh and salt water*, https://tehtab.ru/Guide/GuideMedias/OxigenO_2/OxygenSolubility/ (in Russian).
22. N.A. Karastelev, Kinetics of oxidation of Fe(II) sulfate at high temperatures in an autoclave, *Tekhnicheskie nauki – ot teorii k praktike (Technical sciences - from theory to practice)*, 2016, **53**, 99–105 (in Russian).

♦ ♦ ♦